Development of stereotaxic recording methods for awake marmosets

Wakabayashi, Masahiro

Doctor of Philosophy

Department of Physiological Sciences
School of Life Science

SOKENDAI
(The Graduate University for Advanced Studies)

Contents

Abstract

The common marmoset (*Callithrix jacchus*) is a New World monkey species living in the South America. Marmosets are easier to handle than macaque monkeys, because marmosets are small and gentle. Although the marmoset brain is small and the cerebral cortex is lissencephalic, marmosets share common brain structures with the other primates including macaques and humans. Moreover, their breeding efficacy is high, and this advantage has enabled the generation of transgenic marmosets. Owing to these advantages, marmosets have emerged as an alternative to macaque monkeys as a primate model for neuroscience and medical research. However, there are only a few reports in which neuronal activity was recorded in behaving and awake marmosets. Here, I introduced a newly developed stereotaxic system for marmosets and performed neuronal recording in the awake state.

I modified the head-fixation system for macaque monkeys to fit to marmosets: The metal frame held anterior-posterior stereotaxic bars and head-fixation blocks, and the marmoset chair was composed of neck and waist plates, a perch and a waste tray, which are held by four pillars. Under inhalation anesthesia with 1-2% sevoflurane and 25% N_2O, the head of the marmoset was fixed in a stereotaxic frame. The skull was widely exposed and covered with bone adhesive resin. A pair of head-fixation tubes, which were made from polyether ether ketone, were positioned medio-laterally and horizontally to the stereotaxic plane on the skull and fixed using dental resin. Vital signs were monitored with a pulse oximeter.

After full recovery from the first operation, a structural magnetic resonance imaging (MRI) was acquired by a 3T MRI scanner to localize deep brain structures. Under

general anesthesia with ketamine and xylazine hydrochlorides, the head of the marmoset was fixed painlessly to the stereotaxic MRI apparatus, which was made from materials compatible with MRI and fitted to the inside the volume coil of the scanner.

In order to access the cerebral cortex and deep brain structures, partial craniotomy was performed. A marmoset was seated in the marmoset chair, and its head was painlessly fixed to the stereotaxic frame. Under the general anesthesia with ketamine hydrochloride, the skull was slowly and carefully exfoliated using an ultrasonic scalpel to minimize surgical damage to the brain. Then, the recording chamber was attached to cover the hole and fixed.

To record neuronal activity, the awake marmoset was seated in the marmoset chair with its head restrained. The homemade glass-coated Elgiloy-alloy microelectrode (0.8–1.5 MΩ at 1 kHz) was inserted into the cortex perpendicularly to the cortical surface through the dura mater with a hydraulic microdrive. Neuronal activity was amplified using a homemade amplifier and continuously monitored with an oscilloscope and a sound monitor. Neuronal responses to somatosensory stimuli were examined. Intracortical microstimulation (ICMS; < 60 μA with a train of 12 cathodal monophasic pulses, 200 μs duration at 333 Hz) was performed, and evoked movements and muscle contractions were observed. ICMS typically induced movement of a single joint in the contralateral forelimb, hindlimb, or muscle twitch in the face area. The area where low current stimulation < 10 μA induced movements was found and considered to be the primary motor cortex (MI). In the medial part of the MI, ICMS evoked movements of the hindlimb. The sites representing the forelimb were widely distributed in the area lateral to the hindlimb representation. In the area anterior to the MI, higher current stimulation of 20-50 μA was needed to evoke movements. The area

was considered to be the premotor cortex. The area that required higher current stimulation of 15-30 μA to elicit body movements was found immediately posterior to the MI and was considered as the somatosensory area 3a.

Based on MRI images, the Elgiloy-alloy microelectrode was inserted vertically into the deep brain structures. I successfully recorded in the internal and external segments of the globus pallidus, thalamus, and cerebellar nuclei, which were confirmed by their characteristic firing rates and patterns. I also injected an adeno-associated virus vector carrying the enhanced green fluorescent protein (EGFP) transgene into the caudate nucleus. The expressed EGFP was clearly observed in the nucleus.

This system is suitable for functional mapping of the brain, since the large recording chamber allows stereotaxically access to arbitrary regions over almost the entire brain. In addition, this system is desirable for neuronal recording during task performance to assess motor skills and cognitive function, as the marmoset sits in the marmoset chair and can freely use its hands. Moreover, this system can be used in combination with cutting-edge techniques, such as two-photon imaging and optogenetic manipulation. This recording system will contribute to boosting neuroscience and medical research using marmosets.

1. Introduction

The common marmoset (*Callithrix jacchus*) is a New World monkey species living in the forest of north-eastern Brazil. Marmosets are easier to handle than macaque monkeys, which are the most commonly used primate model for neuroscience and medical research. Marmosets are small (typical adult body weight, 300-500 g) and gentle, and no lethal zoonotic diseases transmissible to human have been reported. They are social animals and share behavioral characteristics with humans, e.g. living in family units, using vocal communication and making eye contact (Cyranoski, 2014; Miller et al., 2016). Although the marmoset brain is much smaller and the cerebral cortex is lissencephalic with undeveloped sulci, marmosets share common brain structures with other primates including macaques and humans. The marmoset brain, unlike rodent brains, has a well-developed prefrontal cortex responsible for cognitive functions (Burman et al., 2006, 2011; Burman and Rosa, 2009; Roberts et al., 2007). The primary motor cortex (MI) and somatosensory cortex are clearly separated (Burman et al., 2008). The motor cortex comprises the MI, premotor cortex (PM) and supplementary motor area (Burman et al., 2008; Burish et al., 2008; Bakola et al., 2015). The somatosensory, visual, and auditory cortices are also well-developed (Krubitzer and Kaas, 1990; de la Mothe et al., 2006; Burish et al., 2008; Solomon and Rosa, 2014; Mitchell and Leopold, 2015). The striatum is divided into the caudate nucleus and putamen by corticofugal fibers (Roberts et al., 2007; Kondo et al., 2015). Moreover, marmosets have ability to learn and perform a variety of tasks to assess motor skills (Tia et al., 2017) and cognitive functions such as visual discrimination (Maclean et al., 2001; Takemoto et al., 2015), reversal learning (Clarke et al., 2005; Rygula et al., 2010;

Takemoto et al., 2015) and decision making (Tokuno and Tanaka, 2011). The compact and lissencephalic features of the marmoset brain are suitable for imaging studies of the cortex, because they allow access to the entire cortical region (Sadakane et al., 2015a, b). Moreover, their breeding efficacy is high due to their short gestation period (about 5 months) and ability to routinely bear twins or triplets, and this advantage has enabled the generation of transgenic marmosets with germline transmission (Sasaki et al., 2009). The whole-genome sequence has recently been provided (Marmoset Genome Sequencing and Analysis Consortium, 2014; Sato et al., 2015) and the development of genome-editing technologies (Sato et al., 2016) has accelerated expectations for the generation of various types of genetically modified marmoset models. Furthermore, a transgenic marmoset model of polyglutamine diseases has recently been reported (Tomioka et al., 2017). Owing to these advantages, marmosets have emerged as an alternative to macaque monkeys as a primate model for neuroscience and medical research (Tokuno et al., 2015; Okano et al., 2016).

Stereotaxic neuronal recording in behaving or awake macaque monkeys under the head-fixed condition has been intensively conducted to examine brain functions since the 1960s, and an increasing amount of knowledge on neural mechanisms underlying motor control (Evarts, 1968; Tanji and Evarts, 1976; Georgopoulos et al., 1982; Nambu et al., 1991; Takara et al., 2011), cognitive functions (Isomura et al., 2003; Minamimoto et al., 2005; Arimura et al., 2013), and neurological disorders (Bergman et al., 1994; Tachibana et al., 2011) has been accumulated. Neuronal recording in behaving/awake rodents under the head-fixed condition has also been developed and rapidly become popular. A lot of studies using behaving rats (Welsh et al., 1995; Bermejo et al., 2004; Hentschke et al., 2006; Stüttgen et al., 2006; Stüttgen and Schwarz 2008; Kimura et al.,

2012; Soma et al., 2017) and mice (O'Connor et al., 2010), and awake mice (Chiken et al., 2008, 2015; Sano et al., 2013) have contributed to understanding of neural mechanisms underlying motor control and sensorimotor integration. In addition, head-fixed behaving/awake mice have been used for two-photon imaging studies (Komiyama et al., 2010; O'Connor et al., 2010) and optogenetic manipulation (Hira et al., 2009; Roseberry et al., 2016; Ozaki et al., 2017). On the other hand, in marmosets, there are only a few reports in which neuronal recordings were conducted in freely moving marmosets (Roy et al., 2016; Nummela et al., 2017), head-fixed awake marmosets for auditory studies (Wang et al., 2005; Gao et al., 2016), or anesthetized marmosets fixed in a stereotaxic frame (Lui et al., 2013; Yu et al., 2013; McDonald et al., 2014). One reason why there are only a few reports on recordings from awake marmosets is that stereotaxic neuronal recording system for behaving/awake marmosets has not been developed. Considering these characteristics of marmosets, a stereotaxic recording system for marmosets, which does not require general anesthesia, will become a strong tool in neuroscience. Here, I introduce a newly developed stereotaxic neuronal recording system for marmosets. A set of the apparatus that contains a marmoset chair, metal frame for the stereotaxic apparatus, head-fixation apparatus, and recording chamber was developed by modifying that for macaque monkeys. A head-fixation apparatus compatible with magnetic resonance imaging (MRI) was also developed to localize deep brain structures, as MRI is routinely used for macaque monkey studies. Using this system, I recorded neuronal activity from the cerebral cortex of awake marmosets, and applied intracortical microstimulation (ICMS) to identify the MI. I also successfully recorded neuronal activities in the subcortical targets, such as the basal ganglia, thalamus, and cerebellum of awake marmosets.

2. Materials and methods

2.1. Animals

Three adult common marmosets (*Callithrix jacchus*; three females; body weight, 350-360 g; CLEA, Tokyo, Japan) were used in the present study. All experimental protocols were approved by the Institutional Animal Care and Use Committee of the National Institutes of Natural Sciences, and all experiments were conducted according to the guidelines of the National Institutes of Health *Guide for the Care and Use of Laboratory Animals*. Animals were trained daily to sit in the marmoset chair under experimental conditions described below. Marmosets were given ad libitum access to food and water.

2.2. Marmoset head-fixation system

For experiments on macaque monkeys including Japanese monkeys in the awake state, a metal frame holding a stereotaxic frame and a macaque monkey chair were used (Nambu et al., 2000). The system for macaque monkeys was modified to fit to marmosets. This marmoset head-fixation system was composed of a metal frame holding a stereotaxic frame (Fig. 1A, B, a-c) and a marmoset chair (Fig. 1A, B, d-h). The metal frame (Fig. 1A, B, c) held anterior-posterior (AP) stereotaxic bars (a) (Narishige, Tokyo, Japan) and head-fixation blocks (b). The marmoset chair was composed of neck (Fig. 1A, B, d) and waist (e) plates, a perch (f) and a waste tray (g), which were held by four pillars (h). The neck and waist plates were made from

transparent polyvinyl chloride to permit easy viewing of a marmoset in the chair. A marmoset was seated on the perch, with the trunk and neck gently held by the neck and waist plates (Fig. 1B). The neck plate could be tilted up to 30° to avoid pressure on the shoulder and jaw of the marmoset (Fig. 1A). The marmoset chair was set inside the metal frame, and the head of the marmoset was painlessly fixed to the AP stereotaxic bars using head-fixation blocks (Fig. 1B). Manipulators were set at the AP bars of the stereotaxic frame, and any regions in the brain could be accessed stereotaxically.

2.3. Head-fixation tube and recording chamber

A pair of head-fixation tubes (Fig. 2A) and a recording chamber (Fig. 2B), which were fixed to the marmoset's skull (Fig. 2C), were made from plastic for MRI compatibility and light weight (total weight was 4.5 g).

The head-fixation tubes were made from polyether ether ketone (PEEK). A PEEK tube with a 6-mm outer-diameter and a 3-mm inner-diameter was cut to 20-mm length (Fig. 2A). In order to fix them firmly to the marmoset's skull by resin and reduce their weight, the upper and lower walls of the tubes, except for 5 mm on both ends, were scraped by 0.8 mm using a milling machine. Total weight of a pair of fixation tubes was 1.2 g.

A recording chamber was made from polyoxymethylene (POM). A 5-mm-thick POM plate was used (Fig. 2B, left). The outer rim (25 mm x 25 mm) and inner rim (19 mm x 19 mm) were milled by using a numerically controlled milling machine (CAMM-3 PNC-3100, Roland, Hamamatsu, Japan). Holes at four corners were drilled

and tapped for M 2.6-mm screws. The weight of a chamber was 1.7 g. The lid of the chamber was made from polycarbonate (PC). A 2-mm-thick transparent PC plate was cut to a 25 mm x 25 mm square (Fig. 2B, right). Holes with a 2.6-mm diameter were drilled at the four corners for M 2.6-mm screws. The weight of a lid was 1.2 g. Small notches were made at the rims of the chamber and lid to show their directions. The lid was fixed to the chamber by four M 2.6-mm PEEK screws with a total weight of 0.4 g.

2.4. Surgical procedure for head fixation

Under general anesthesia, marmosets received a surgical operation to fix their heads painlessly to the stereotaxic frame. Anesthesia was induced with intramuscular injection of ketamine hydrochloride (25 mg/kg body weight) and xylazine hydrochloride (2 mg/kg). Atropine sulfate (5 μg) was also intramuscularly administered to reduce airway mucus secretion. Then, the marmoset was fixed in a stereotaxic frame (Narishige) with a mouthpiece, two ear bars and two eye pieces. The mouth and nose of the marmoset were covered by a homemade face mask. The mask was made of a bottom part of 50-ml disposable tube, a silicon rubber membrane (KE-1603, Shin-Etsu Chemical, Tokyo, Japan.), and two connectors, which were fixed with a urethane-based adhesive. All materials were transparent to permit easy viewing of marmoset's mouth and nose (Fig. 2D). The mouthpiece was inserted to the mouth through the mask and covered with a silicon rubber. The gap between the marmoset's jaw and the mask was covered with a silicon membrane (Fig. 2E). The marmoset breathed spontaneously, and a mixture of 25% N_2O, 25% O_2, and 50% room air with

1-2% sevoflurane was supplied by an inhalation anesthesia machine (MK-AT210, Muromachi Kikai, Tokyo, Japan) to the mask at 2,000 ml/min. Vital signs, such as heart rates and arterial oxygen saturation (SpO_2), were monitored with a pulse oximeter (OLV-2700, Nihon Kohden, Tokyo, Japan). Sensors for SpO_2 (TL-260T, Nihon Kohden) were attached to the plantar of the marmoset. Heart rates and SpO_2 were kept 80-120 beats/min and > 90%, respectively. The body temperature of the marmoset was controlled by a heating pad (MP-912, Torio, Osaka, Japan) and an aluminum-metallized film (emergency sheet gold, Logos, Osaka, Japan).

The skin of the marmoset's head was incised, and the skull was widely exposed. The temporal muscle, periosteum, and blood were completely removed. Hemorrhage from the bone was treated by crushing bone with a dental drill and sealing with bone wax (Lukens, NM, USA). The exposed skull was decalcified with 10% citric acid for a minute and 0.3% hypochlorous acid for a minute, and then washed with saline. A non-magnetic titanium screw (M2.6, 8 mm length) for the ground was implanted into the lateral part of the supraorbital ridge. The exposed skull was covered with bone adhesive resin (Bistite II, Tokuyama Dental, Tokyo, Japan). In macaque monkeys, around ten PEEK screws (M3, 5mm length) were screwed into the skull as anchors. On the other hand, bone adhesive resin fixed a marmoset head strongly enough without anchor screws. For stereotaxic approaches, a titanium pin (φ 0.5 mm) was fixed as a reference point. The tip of the pin was set 20 mm dorsal to the interaural midpoint of the Horsley-Clark stereotaxic coordinates using dental resin (Unifast II, GC, Tokyo, Japan). A pair of head-fixation tubes were positioned medio-laterally and horizontally to the Horsley-Clark stereotaxic plane on the skull and fixed using dental resin (Fig. 2C). All surgical procedures were performed under aseptic conditions. This surgery

typically took 2-3 hours. Antibiotics (minocycline, 5 mg/kg) and analgesics (ketoprofen, 2 mg/kg) were intramuscularly administered for 2-3 days after the surgery.

2.5. MRI scanning of the marmoset brain

After full recovery from the first operation, a structural MRI was acquired by a 3T MRI scanner (3T Allegra; Siemens, Erlangen, Germany) to localize deep brain structures. The stereotaxic apparatus was made from materials compatible with MRI and fitted to the inside the volume coil of the scanner (Fig. 3A). The apparatus was composed of two supporting structures (Fig. 3A, a), a stereotaxic MRI frame (b), two fixation blocks (c), two titanium rods (d), and a grid showing stereotaxic coordinates (e). They were made from acrylic resin (a, b, e) or POM (c). After general anesthesia with ketamine hydrochloride (25 mg/kg, i.m.) and xylazine hydrochloride (2 mg/kg, i.m.), the head of the marmoset was fixed painlessly to the stereotaxic MRI apparatus. Two titanium rods (φ 3 mm) were inserted into fixation tubes on the marmoset's head and fixed to the head-fixation blocks of the stereotaxic apparatus with adhesive silicon (MEMOSIL, Kulzer, Hanau, Germany). The grid (Fig. 3A, e) was filled with contrast medium (Omniscan 32%, GE Healthcare, IL, USA) and agarose in a 1 cm x 1 cm grid pattern, and positioned based on the stereotaxic plate coordinates. Heart rate and SpO_2 were monitored using an MRI-compatible fiber oximeter (7500FO, Nonin Medical, MN, USA). Then, MRI scanning was performed (Fig. 3B). The parameters for MRI scanning were 3D-MPRAGE, 192 axial slices, 0.8-mm thickness, TR/TE = 2500/5.16 ms, 144 x 192 matrix size, and yielding to isotropic voxels of 0.8 mm.

2.6. Craniotomy and chamber fixation

In order to access the cerebral cortex and deep brain structures (Palazzi and Bordier, 2008; Paxinos et al., 2010), partial craniotomy was performed and the recording chamber was fixed. A marmoset was seated in the marmoset chair. The marmoset head was painlessly fixed to the stereotaxic frame. Two stainless steel rods (φ 3 mm) were inserted into fixation tubes on the marmoset's head and fixed to the head-fixation blocks of the stereotaxic frame (Figs. 1B and 2C). Under the general anesthesia with ketamine hydrochloride (25 mg/kg, i.m.), the resin that covered the skull over the target area was removed by a dental drill (Volver Vmax, NSK, Tochigi, Japan), and the skull was exposed. Cerebral edema was more often induced in marmosets compared to macaque monkeys. To minimize surgical damage to the brain, an ultrasonic scalpel (Piezosurgery®touch, Mectron, Carasco, Italy) was used. Compared with a conventional dental drill, the ultrasonic scalpel has the following advantages (Kotrikova et al., 2006): (1) The micro-vibrations of instruments at ultrasonic frequency can smash or cut the target bone, but does not damage soft tissues, such as dura mater and brain tissue; (2) The ultrasonic scalpel induces little heat and avoids thermal damage to tissues; and (3) The cavitation effect of ultrasound minimizes bleeding from the bone. The skull was slowly and carefully exfoliated using the ultrasonic scalpel. Hemorrhage from the dura mater was treated with a mixture of 2% lidocaine and 0.00125% epinephrine (xylocaine cartridge for dental use, DENTSPLY, Tokyo, Japan). After removal of the skull over the target area, the recording chamber was attached to cover the hole (Fig. 2B, C), and fixed using resin (Unifast II). After the inside was washed with saline, the chamber was covered by the lid. To prevent infection, the

inside of the chamber was washed at least 2-3 times a week.

2.7. Recording electrodes

Homemade glass-coated Elgiloy-alloy microelectrodes were used for recording and microstimulation. For macaque monkeys, Elgiloy-alloy wire of 0.558 mm in diameter (E00204, Rocky Mountain Orthodontics, CO, USA) was etched and covered with solder glass (SGL-1, Narishige; Nambu et al., 2000). For marmosets, thinner wire, such as 0.254 mm or 0.356 mm in diameter (E00210 and E00214, respectively, Rocky Mountain Orthodontics) was used. The impedance of the electrode was 0.8–1.5 MΩ at 1 kHz.

2.8. Electrophysiological mapping of the cerebral cortex

The awake marmoset was seated in the marmoset chair. A pair of metal rods was inserted into the head-fixation tubes, and the head of the marmoset was painlessly fixed to the stereotaxic frame (Figs. 1B and 2C). The lid of the chamber was temporarily removed. A glass-coated Elgiloy-alloy microelectrode was inserted perpendicularly to the cortical surface through the dura mater into the cortex with a hydraulic microdrive (MO-81, Narishige). Neuronal activity was amplified (5,000 times) using a homemade amplifier, filtered (200-5,000 Hz), and continuously monitored with an oscilloscope and a sound monitor. Extracellular unit activity was recorded at 200- to 500-μm intervals, and then sampled at 20k-50k Hz with a computer. Neuronal responses to somatosensory stimuli (skin touch and passive joint movement) in the

orofacial part (lip and jaw), contralateral forelimb (digit, wrist, elbow, and shoulder) and hindlimb (ankle, knee, and hip) were examined. Following extracellular unit recording, ICMS was performed. Currents of < 60 μA were delivered with a train of 12 cathodal monophasic pulses (200 μs duration at 333 Hz), and evoked movements and muscle contractions of various body parts were carefully observed.

2.9. Adeno-associated virus (AAV) vector injection

An AAV-DJ vector carrying the enhanced green fluorescent protein (EGFP) transgene (AAVDJ-CAGGS-EGFP) was packaged using AAV Helper Free Expressing System (Cell Biolabs, Inc, CA, USA) and purified as described previously (Kobayashi et al., 2016). In brief, the packaging plasmid (pAAV-DJ and pHelper) and transfer plasmid (pAAV-CAGGS-EGFP, Addgene #22212) were transfected to HEK293T cells by the calcium phosphate method. The harvested cells were lysed by repeated and thawing, and the crude cell extract containing AAV vector particles was obtained. AAV vector particles were purified by serial ultracentrifugation with cesium chloride. The purified particles were dialyzed with PBS (phosphate buffered saline), and then concentrated by ultrafiltration. The copy number of viral genomes (vg) was determined by the TaqMan Universal Master Mix II (Applied Biosystems, CA, USA) with the following primers and probe: 5'-CCGTTGTCAGGCAACGTG-3', 5'-AGCTGACAGGTGGTGGCAAT-3' and 5'- TGCTGACGCAACCCCCACTGGT -3'.

The AAV vector (0.3 μl) was pressure-injected into caudate nucleus, a part of input stations of the basal ganglia, using a 10-μl microsyringe (1701N, Hamilton, NV, USA).

After 15 minutes of waiting time, the needle was removed. When bleeding occurred at the injection point, astriction was performed.

2.10. Recording from the deep brain structures

Based on the MRI images and the marmoset brain atlas (Palazzi and Bordier, 2008; Paxinos et al., 2010), a glass-coated Elgiloy-alloy microelectrode was inserted vertically into the basal ganglia, thalamus, and cerebellum with a hydraulic microdrive (MO-81, Narishige) in the awake state following the method used in macaque monkeys (Nambu et al., 1988, 1990). Activity of a single neuron was isolated. The activity of the following structures was recorded: the external (GPe) and internal (GPi) segments of the globus pallidus (GP), thalamus, and deep cerebellar nuclei (CN). Each brain structure could be identified by depth profiles of recording activity and firing rates and patterns.

2.11. Histological analyses

After a survival period of 3 weeks from AAV voctor injection, marmosets were deeply anesthetized with sodium pentobarbital (50 mg/kg, i.p.) and perfused transcardially with 0.1 M phosphate buffer (PB, pH 7.3) followed by 10% formalin in 0.1 M PB, and the same buffer containing 10% sucrose and, finally, 30% sucrose. The brain was extracted and kept in 0.1 M PB containing 30% sucrose at 4°C. It was cut serially into 50-μm-thick frontal sections on a freezing microtome. The sections were divided into two groups. The first group was mounted onto gelatin-coated glass slides

and stained with Cresyl violet. The sections of the second group were processed immunohistochemistry to visualize expressed GFP. The sections were incubated in 0.1 M PBS, containing 0.4% Triton X-100 and a primary antibody, rabbit anti-GFP antibody (1:1000; Molecular Probes, Eugene, OR) for overnight at 4°C. Then the sections were incubated with a biotinylated secondary antibody, anti-rabbit IgG (1:200; BA-1000, Vector Laboratories, CA, USA) for 3 hours at room temperature, followed by fresh PBS containing avidin-biotin-peroxidase complex (PK-6100, Vector Laboratories) for 1.5 hours. Subsequently, the sections were reacted for 10–20 minutes in 0.1 M PBS containing 0.04% diaminobenzidine and 0.003% H_2O_2. The sections reacted for GFP were mounted onto gelatin-coated glass slides, then observed under a light microscope.

3. Results

3.1. Condition of marmosets after surgery

After surgery for installation of the head-fixation tubes and recording chamber using these surgical procedures, all three marmosets remained in good health. Inhalational anesthesia with sevoflurane largely contributed to reducing the physical damage from surgery, because of the following advantages: short induction and recovery time, no irritation to the respiratory system, and little effect on the cardiovascular system. Marmosets woke up just after surgery and started to eat food on the same day. Craniotomy using an ultrasonic scalpel was also very efficient and successfully exfoliated their skulls without causing cerebral edema. The light-weight head-fixation tubes and recording chamber installed on their skulls did not affect their daily behavior in their home cages.

3.2. Neuronal recording and ICMS mapping of the sensorimotor areas in the cerebral cortex

After one- or two-month training, the marmosets could sit in the marmoset chair quietly with their head restrained in the awake state, and they did not show any signs of discomfort while they were sitting in the chair for 3-4 hours. Marmosets' heads were rigidly fixed to the stereotaxic frame using the head-fixation apparatus. Marmosets could move their hands freely in the chair, but the neck plate of the marmoset chair effectively prevented them from reaching their hands to the recording apparatus. The

bone adhesive and dental resin that fixed head-fixation tubes to the marmosets' skulls were strong, and good recording quality was kept over several minutes even when they moved their arms and legs. The homemade glass-coated Elgiloy-alloy microelectrode was inserted in the sensorimotor region of the cerebral cortex (Fig. 4A) to record neuronal activity and conduct ICMS mapping. Single-unit activity of the cortical neurons was successfully recorded through the microelectrode (Fig. 4B). I could touch their bodies, apply somatosensory stimuli to the hindlimb, forelimb, and face, and successfully detect sensory responses of cortical neurons. ICMS typically induced movement of a single joint in the contralateral forelimb, hindlimb, or muscle twitch in the face area. The area where low current stimulation less than 10 μA induced movements was found (Fig. 4C). I considered it as the MI. In the medial part of the MI, ICMS evoked movements of the hindlimb, such as the hip, knee, and digits of the hindlimb. The sites representing the forelimb, such as the shoulder, elbow, wrist, and digits of the forelimb, were widely distributed in the area lateral to the hindlimb representation. Movements of eyelid were observed by stimulation of the most lateral part in the MI area examined in this study. In the area anterior to the MI, higher current stimulation of 20-50 μA was needed to evoke movements. The area was considered to be the PM. The PM was also somatotopically organized. The area representing the hindlimb was found in the medial part, whereas the area representing the forelimb was found in the lateral part. I also found the area that required higher current stimulation of 15-30 μA to elicit body movements immediately posterior to the MI. The area was considered as the somatosensory area 3a, which is located at the bottom of the central sulcus in macaque monkeys. Similar to the MI and PM, the hindlimb representation was found in the medial part of the area 3a, and the sites

representing the forelimb were widely distributed in the area lateral to the hindlimb representation. In the area posterior to the area 3a, there were sites that required 40 μA or higher current to induce body movements. This area would be the somatosensory area 3b. Histological examination (Fig. 4D, E) showed that the border between the MI and area 3a defined electorophysiologically (a black arrow in Fig 4E) corresponded well to the border defined cytoarchitectonically (white broken lines in Fig. 4E).

3.3. Neuronal recordings in the deep brain structures

The MRI images using the MRI-compatible stereotaxic apparatus were successfully acquired (Fig. 3). Stereotaxic coordinates of target structures were calculated based on MRI images referring to the 1 cm x 1 cm grid and the marmoset brain atlas (Palazzi and Bordier, 2008; Paxinos et al., 2010). The large recording chamber installed on the marmoset's head allowed us to record neuronal activity from several brain regions in each marmoset.

First, the basal ganglia, such as the GPe and GPi were targeted. The target areas were 7.0-8.0 mm anterior (A), 4.5-6.5 mm lateral (L), and 6.5-9.5 mm dorsal (D) to the interaural midpoint for the GPe and A 7.0-8.0 mm, L 3.5-5.8 mm, and D 6.5-8.0 mm for the GPi. The Elgiloy-alloy microelectrode was inserted vertically. After penetrating the dura mater, large spike firings at low frequency were recorded and considered to be originated from cerebral cortical neurons. As the electrode was continuously advanced by 200-500 μm, similar activity was recorded. After a depth of 1,800-2,200 mm, activity became low and the tip of the electrode was considered to be in the white matter or the caudate nucleus. Then, large spike firings at high frequency were suddenly

recorded and considered to be originated from GP neurons (Fig. 5A). Neuronal activity with sustained firings and pauses was recorded in the lateral region of the GP (Fig. 5A, upper), while activity with sustained firings and no pauses was recorded in the medial region (Fig. 5A, lower). The former and the latter were considered to be the activity of the GPe and GPi, respectively, based on their firing characteristics in macaque monkeys (Delong, 1971). The GPe and GPi neurons in Fig. 5A changed their activity during passive movements of elbow joints and thus they were considered to be in the forelimb regions of the GPe/GPi.

Next, recordings of neuronal activity in the motor thalamus (A 5.5-6.3 mm, L 3.0-5.0 mm, D 8.0-11.0 mm) were attempted. The recording electrode was inserted vertically through the cerebral cortex and the caudate nucleus. Then, neuronal activity at the target site was recorded (Fig. 5B). This was considered to be recorded in the motor thalamus because it exhibited rhythmic firings and changed its activity in relation to arm movements (Vitek et al., 1994). Moreover, the CN (Posterior 3.2-4.2 mm, L 2.0-4.5 mm, D 4.5-5.5 mm) was also targeted. The recording electrode was inserted vertically through the visual cortex and white matter. After going through the cerebellum tentorium, neuronal activity in the cerebellar cortex was recorded, which was characterized by complex and simple spikes of Purkinje cells. Finally, the recording electrodes reached the CN (Fig. 5C). This was considered to be recorded in the dentate nucleus, because of large-amplitude continuous firings (Thach, 1968) and its stereotaxic coordinates.

The AAV-DJ vector (0.3 μl, 1.0 x 10^9 copies of vg/μl) was injected into caudate nucleus (A 1.8 mm, L 2.1 mm, D 10.5 mm from interaural midpoint). The expressed GFP was clearly observed in the caudate nucleus (Fig. 4F).

4. Discussion

The common marmoset has been proposed as a potential alternative to macaque monkeys as a primate model for neuroscience and medical research. However, there are only a few reports in which neuronal activity was recorded in behaving and awake marmosets. In the present study, I have newly developed a stereotaxic neuronal recording system for awake marmosets under the head-fixed condition by modifying that for macaque monkeys.

Marmosets are much smaller and easier to handle than macaques. Conversely, they are much weaker than macaques, and minor physical damage and mental stresses often cause a decrease in appetite and enervation. To minimize physical damage, safe surgical procedures for craniotomy and installation of the head-fixation apparatus were contrived. Furthermore, inhalational anesthesia with sevoflurane instead of intravenous or intramuscular injection of anesthetic drugs was adopted using a handmade mask. Inhalational anesthesia with sevoflurane is rapid in onset and offset, so marmosets woke up just after the end of the surgery and could eat on the same day. Bone adhesive resin was used to fix the head-fixation tubes to their skulls instead of anchor screws, which are commonly used in surgery for macaque monkeys, and this procedure could much shorten surgical operation time. Employment of craniotomy using an ultrasonic scalpel enabled to open their skulls without causing cerebral edema. The total weight of the head-fixation tubes and recording chamber was less than 5 g, so the apparatus did not affect their daily behavior in their home cages. As a result, all marmosets remained in good health during several months of the experimental period.

This stereotaxic recording apparatus for marmosets modified from that for macaque

monkeys is very suitable for electrophysiological experiments on awake marmosets because of the following advantages. The marmoset chair is composed of neck and waist plates, a perch, and a waste tray, which are held by four pillars (Fig. 1). Marmosets seemed to sit comfortably in the marmoset chair with their head restrained. No chair plates pressed on their body, and the tiltable neck plate allowed them to eat small pieces of food in the chair. Marmosets could freely move their arms and legs in the chair, and their bodies could be easily touched by an experimenter. The head-fixation apparatus could rigidly fix their heads to the stereotaxic frame. The metal frame holding the stereotaxic frame is firm and allows us stable electrophysiological recording even when marmosets move in the chair. Manipulators set at the AP bars of the stereotaxic frame allowed access to any region in the brain through the large recording chamber (Fig. 2).

Using the apparatus, neuronal activities of the cerebral cortex and conducted ICMS mapping in awake marmosets were recorded. Based on evoked movements by ICMS and neuronal responses to sensory stimuli, the MI, PM, and areas 3a and 3b (Fig. 4) were successfully identified. The threshold for evoking movements in the MI was low (less than 10 μA) and comparable to that in awake macaque monkeys (Sato and Tanji 1989). In ICMS mapping studies of the MI conducted in anesthetized marmosets (Burish et al., 2008; Burman et al., 2008), the threshold of ICMS to evoke movements was 55-120 μA and was much higher than that in awake macaques, and the following possibilities have been suggested for the reasons for the higher threshold: (1) General anesthesia decreases neural excitability; and (2) The cortico-spinal tract does not synapse directly to motoneurons in the spinal cord in the marmoset (Kondo et al., 2015). The present results revealed that the high stimulation threshold in previous studies is

due to the effect of anesthesia. Weak stimulation of the MI could induce movements in marmosets as well as macaque monkeys. The MI and areas 3a and 3b, which are mostly buried in the central sulcus of macaque monkeys, could be easily mapped in marmosets.

The neuronal activities in the deep brain structures such as the basal ganglia, thalamus, and cerebellum were also recorded. MRI images acquired using the MRI-compatible stereotaxic frame were very helpful to target these structures. Based on MRI images, recording electrodes were successfully inserted into the GPe and GPi, motor thalamus, and CN, and recorded single-neuronal activities (Fig. 5). GPe neurons showed high spontaneous activity interrupted by firing pauses, while GPi neurons showed high spontaneous activity without pauses. These firing characteristics are identical to those reported in macaque monkeys and humans (DeLong, 1971; Vitek et al., 1997). Based on the stereotaxic coordination, the AAV-DJ vector was successfully injected into the caudate nucleus, and the expressed GFP was clearly observed in the caudate nucleus (Fig. 4F). Using similar methods, any drugs and viral vectors were injected to stimulate or block in physiologically identified cortical and subcortical areas.

The present stereotaxic recording system is suitable for neuronal recording during task performance of limb and oculomotor movements, since marmosets can move their hands freely and their fixed-heads allows us to easily track their eye movements. Marmosets can learn not only simple motor tasks (Tia et al., 2017) but also various types of tasks to assess cognitive functions, such as visual discrimination (Maclean et al., 2001; Takemoto et al., 2015), reversal learning (Clarke et al., 2005; Rygula et al., 2010; Takemoto et al., 2015) and decision-making (Tokuno and Tanaka, 2011). Thus, neural

mechanisms underlying motor control and cognitive functions can be investigated in marmosets by using the present stereotaxic recording system. In addition, the present stereotaxic recording system can be used for two-photon imaging study. Taking advantage of their compact and lissencephalic brain, two-photon imaging studies have been conducted on awake or anesthetized marmosets (Sadakane et al., 2015a, b; Stantisakultarm et al., 2016; Yamada et al., 2016). Using the present stereotaxic recording system, two-photon imaging under the awake condition and during task performance can be conducted as reported in head-fixed mice (Dombeck et al., 2007; Komiyama et al., 2010). The present stereotaxic recording system is also applicable for optogenetic manipulation. In macaque monkeys, difficulty in optogenetic manipulation of behavior has been suggested (Kinoshita and Isa, 2015). Since macaques have a large brain, the delivery of light with substantial strength to the wide area is required to change their behavior. On the other hand, in the compact brains of marmosets, delivered light should be able to activate proper areas to induce behavioral changes. Recently, various types of genetically modified marmoset models have been expected, and a transgenic marmoset model of polyglutamine diseases has actually been generated (Tomioka et al., 2017). A project to generate marmoset Cre lines through knock-in strategies has also be planned (Okano et al., 2016), which may make cell-type-specific manipulation possible. The present recording system can be used to analyze these types of marmosets and would largely contribute to understanding of neural mechanisms underlying motor control, cognitive functions, and neurological disorders in the near future.

5. Conclusions

A stereotaxic neuronal recording system for awake marmosets under the head-fixed condition was newly developed. The present system is suitable for various experiments, such as functional brain mapping and neuronal recording during task performance. In addition, the system can be used in combination with cutting-edge techniques, such as two-photon imaging and optogenetic manipulation. The recording system reported in this study will boost neuroscience and medical research using marmosets.

Acknowledgements

I thank H. Isogai, M. Goto, S. Sato, and N. Suzuki for technical assistance.

6. References

Arimura, N., Nakayama, Y., Yamagata, T., Tanji, J., Hoshi, E., 2013. Involvement of the globus pallidus in behavioral goal determination and action specification. J. Neurosci. 33, 13639-13653.

Bakola S., Burman K.J., Rosa M.G., 2015. The cortical motor system of the marmoset monkey (*Callithrix jacchus*). Neurosci. Res. 93: 72-81.

Bergman H, Wichmann T, Karmon B, DeLong M.R., 1994. The primate subthalamic nucleus. II. Neuronal activity in the MPTP model of parkinsonism. J. Neurophysiol. 72, 507-520.

Bermejo R., Szwed M., Friedman W., Ahissar E., Zeigler H.P., 2004. One whisker whisking: unit recording during conditioned whisking in rats. Somatosens. Mot. Res. 21, 183-187.

Burish M.J., Stepniewska I., Kaas J.H., 2008. Microstimulation and architectonics of frontoparietal cortex in common marmosets (*Callithrix jacchus*). J. Comp. Neurol. 507, 1151-1168.

Burman K.J., Palmer S.M., Gamberini M., Rosa M.G., 2006. Cytoarchitectonic subdivisions of the dorsolateral frontal cortex of the marmoset monkey (*Callithrix jacchus*), and their projections to dorsal visual areas. J. Comp. Neurol. 495, 149-172.

Burman K.J., Palmer S.M., Gamberini M., Spitzer M.W., Rosa M.G., 2008. Anatomical and physiological definition of the motor cortex of the marmoset monkey. J. Comp. Neurol. 506, 860-876.

Burman K.J., Rosa M.G., 2009. Architectural subdivisions of medial and orbital frontal cortices in the marmoset monkey (*Callithrix jacchus*). J. Comp. Neurol. 514, 11-29.

Burman K.J., Reser D.H., Yu H.H., Rosa M.G., 2011. Cortical input to the frontal pole of the marmoset monkey. Cereb. Cortex 21, 1712-1737.

Chiken S., Shashidharan P., Nambu A., 2008. Cortically evoked long-lasting inhibition of pallidal neurons in a transgenic mouse model of dystonia. J. Neurosci. 28, 13967-13977.

Chiken S., Sato A., Ohta C., Kurokawa M., Arai S., Maeshima J., Sunayama-Morita T., Sasaoka T., Nambu A., 2015. Dopamine D1 receptor-mediated transmission maintains information flow through the cortico-striato-entopeduncular direct pathway to release movements. Cereb. Cortex 25, 4885-4897.

Clarke H.F., Walker S.C., Crofts H.S., Dalley J.W., Robbins T.W., Roberts A.C., 2005. Prefrontal serotonin depletion affects reversal learning but not attentional set shifting. J. Neurosci. 25, 532-538.

Cyranoski D., 2014. Marmosets are stars of Japan's ambitious brain project. Nature 514, 151-152.

de la Mothe L.A., Blumell S., Kajikawa Y., Hackett T.A., 2006. Cortical connections of the auditory cortex in marmoset monkeys: core and medial belt regions. J. Comp. Neurol. 496, 27-71.

DeLong M.R., 1971. Activity of pallidal neurons during movement. J. Neurophysiol. 34, 414-427.

Dombeck D.A., Khabbaz A.N., Collman F., Adelman T.L., Tank D.W., 2007. Imaging large-scale neural activity with cellular resolution in awake, mobile mice. Neuron 56, 43-57.

Evarts E.V., 1968. A technique for recording activity of subcortical neurons in moving animals. Electroencephalogr. Clin. Neurophysiol. 24, 83-86.

Gao L, Kostlan K, Wang Y, Wang X., 2016. Distinct subthreshold mechanisms underlying rate-coding principles in primate auditory cortex. Neuron. 91, 905-919.

Georgopoulos A.P., Kalaska J.F., Caminiti R., Massey J.T., 1982. On the relations between the direction of two-dimensional arm movements and cell discharge in primate motor cortex. J. Neurosci. 2, 1527-1537.

Hentschke H., Haiss F., Schwarz C., 2006. Central signals rapidly switch tactile processing in rat barrel cortex during whisker movements. Cereb. Cortex 16, 1142-1156.

Hira R., Honkura N., Noguchi J., Maruyama Y., Augustine G.J., Kasai H., Matsuzaki M., 2009. Transcranial optogenetic stimulation for functional mapping of the motor cortex. J. Neurosci. Methods 179, 258-263.

Isomura Y., Ito Y., Akazawa T., Nambu A., Takada M., 2003. Neural coding of "attention for action" and "response selection" in primate anterior cingulate cortex. J. Neurosci. 23, 8002-8012.

Kimura R., Saiki A., Fujiwara-Tsukamoto Y., Ohkubo F., Kitamura K., Matsuzaki M., Sakai Y., Isomura Y., 2012. Reinforcing operandum: rapid and reliable learning of skilled forelimb movements by head-fixed rodents. J. Neurophysiol. 108, 1781-1792.

Kinoshita M., Isa T., 2015. Potential of optogenetics for the behavior manipulation of non-human primates. In: Optogenetics. Light-sensing proteins and their application, pp 279-290. Tokyo: Springer Japan.

Kobayashi K., Sano H., Kato S., Kuroda K., Nakamuta S., Isa T., Nambu A., Kaibuchi K., Kobayashi K., 2016. Survival of corticostriatal neurons by Rho/Rho-kinase signaling pathway. Neurosci. Lett. 630, 45-52.

Komiyama T., Sato T.R., O'Connor D.H., Zhang Y.X., Huber D., Hooks B.M., Gabitto M., Svoboda K., 2010 Learning-related fine-scale specificity imaged in motor cortex circuits of behaving mice. Nature 464, 1182-1186.

Kondo T., Yoshihara Y., Yoshino-Saito K., Sekiguchi T., Kosugi A., Miyazaki Y., Nishimura Y., Okano H.J., Nakamura M., Okano H., Isa T., Ushiba J., 2015. Histological and electrophysiological analysis of the corticospinal pathway to forelimb motoneurons in common marmosets. Neurosci. Res. 98, 35-44.

Kotrikova B., Wirtz R., Krempien R., Blank J., Eggers G., Samiotis A., Mühling J., 2006. Piezosurgery—a new safe technique in cranial osteoplasty? Int. J. Oral. Maxillofac. Surg. 35, 461-465.

Krubitzer L.A., Kaas J.H., 1990. The organization and connections of somatosensory cortex in marmosets. J. Neurosci. 10, 952-974.

Lui L.L., Bourne J.A., Rosa M.G., 2013. Relationship between size summation properties, contrast sensitivity and response latency in the dorsomedial and middle temporal areas of the primate extrastriate cortex. PLoS One 8, e68276.

Maclean C.J., Gaffan D., Baker H.F., Ridley R.M., 2001. Visual discrimination learning impairments produced by combined transections of the anterior temporal stem, amygdala and fornix in marmoset monkeys. Brain Res. 888, 34-50.

Marmoset Genome Sequencing and Analysis Consortium, 2014. The common marmoset genome provides insight into primate biology and evolution. Nat. Genet. 46, 850-857.

McDonald J.S., Clifford C.W., Solomon S.S., Chen S.C., Solomon S.G., 2014. Integration and segregation of multiple motion signals by neurons in area MT of primate. J. Neurophysiol. 111, 369-378.

Miller C.T., Freiwald W.A., Leopold D.A., Mitchell J.F., Silva A.C., Wang X., 2016. Marmosets: A neuroscientific model of human social behavior. Neuron 90, 219-233.

Minamimoto T., Hori Y., Kimura M., 2005. Complementary process to response bias in the centromedian nucleus of the thalamus. Science. 308, 1798-1801.

Mitchell J.F., Leopold D.A., 2015. The marmoset monkey as a model for visual neuroscience. Neurosci. Res. 93, 20-46.

Nambu A., Yoshida S., Jinnai K., 1988. Projection on the motor cortex of thalamic neurons with pallidal input in the monkey. Exp. Brain Res. 71, 658-662.

Nambu A., Yoshida S., Jinnai K., 1990. Discharge patterns of pallidal neurons with input from various cortical areas during movement in the monkey. Brain Res. 519, 183-191.

Nambu A., Yoshida S., Jinnai K., 1991. Movement-related activity of thalamic neurons with input from the globus pallidus and projection to the motor cortex in the monkey. Exp. Brain Res. 84, 279-284.

Nambu A., Tokuno H., Hamada I., Kita H., Imanishi M., Akazawa T., Ikeuchi Y., Hasegawa N., 2000. Excitatory cortical inputs to pallidal neurons via the subthalamic nucleus in the monkey. J. Neurophysiol. 84, 289–300

Nummela S.U., Jovanovic V., de la Mothe L., Miller C.T., 2017. Social Context-Dependent Activity in Marmoset Frontal Cortex Populations during Natural Conversations. J. Neurosci. 37, 7036-7047.

O'Connor D.H., Peron S.P., Huber D., Svoboda K., 2010. Neural activity in barrel cortex underlying vibrissa-based object localization in mice. Neuron 67, 1048-1061.

Okano H., Sasaki E., Yamamori T., Iriki A., Shimogori T., Yamaguchi Y., Kasai K., Miyawaki A., 2016. Brain/MINDS: A Japanese National Brain Project for Marmoset Neuroscience. Neuron 92, 582-590.

Ozaki M., Sano H., Sato S., Ogura M., Mushiake H., Chiken S., Nakao N., Nambu A., 2017. Optogenetic activation of the sensorimotor cortex reveals "local inhibitory and global excitatory" inputs to the basal ganglia. Cereb. Cortex 27, 5716-5726.

Palazzi X., Bordier N., 2008. The marmoset brain stereotaxic coordinates. NY: Springer.

Paxinos G., Watson C., Petrides M., Rosa M., Tokuno H., 2010. The marmoset brain stereotaxic coordinates. London: Academic Press.

Roberts A.C., Tomic D.L., Parkinson C.H., Roeling T.A., Cutter D.J., Robbins T.W., Everitt B.J., 2007. Forebrain connectivity of the prefrontal cortex in the marmoset monkey (*Callithrix jacchus*): an anterograde and retrograde tract-tracing study. J. Comp. Neurol. 502, 86-112.

Roseberry T.K., Lee A.M., Lalive A.L., Wilbrecht L., Bonci A., Kreitzer A.C., 2016. Cell-type-specific control of brainstem locomotor circuits by basal ganglia. Cell 164, 526-537.

Roy S., Zhao L., Wang X., 2016. Distinct neural activities in premotor cortex during natural vocal behaviors in a new world primate, the common marmoset (*Callithrix jacchus*). J. Neurosci. 36, 12168-12179.

Rygula R., Walker S.C., Clarke H.F., Robbins T.W., Roberts A.C., 2010. Differential contributions of the primate ventrolateral prefrontal and orbitofrontal cortex to serial reversal learning. J. Neurosci. 30, 14552-14559.

Sadakane O., Masamizu Y., Watakabe A., Terada S., Ohtsuka M., Takaji M., Mizukami H., Ozawa K., Kawasaki H., Matsuzaki M., Yamamori T., 2015a, Long-term two-photon calcium imaging of neuronal populations with subcellular resolution in adult non-human primates. Cell Rep. 13, 1989-1999.

Sadakane O., Watakabe A., Ohtsuka M., Takaji M., Sasaki T., Kasai M., Isa T., Kato G., Nabekura J., Mizukami H., Ozawa K., Kawasaki H., Yamamori T., 2015b. In Vivo Two-Photon Imaging of Dendritic Spines in Marmoset Neocortex (1,2,3). eNeuro 2, 4.

Santisakultarm T.P., Kersbergen C.J., Bandy D.K., Ide D.C., Choi S.H., Silva A.C. 2016. Two-photon imaging of cerebral hemodynamics and neural activity in awake and anesthetized marmosets. J Neurosci Methods, 271, 55-64.

Sano H., Chiken S., Hikida T., Kobayashi K., Nambu A., 2013. Signals through the striatopallidal indirect pathway stop movements by phasic excitation in the substantia nigra. J. Neurosci. 33, 7583-7594.

Sasaki E., Suemizu H., Shimada A., Hanazawa K., Oiwa R., Kamioka M., Tomioka I., Sotomaru Y., Hirakawa R., Eto T., Shiozawa S., Maeda T., Ito M., Ito R., Kito C., Yagihashi C., Kawai K., Miyoshi H., Tanioka Y., Tamaoki N., Habu S., Okano H., Nomura T., 2009. Generation of transgenic non-human primates with germline transmission. Nature 459, 523-537.

Sato K., Kuroki Y., Kumita W., Fujiyama A., Toyoda A., Kawai J., Iriki A., Sasaki E., Okano H., Sakakibara Y., 2015. Resequencing of the common marmoset genome improves genome assemblies and gene-coding sequence analysis. Sci. Rep. 5, 16894.

Sato K., Oiwa R., Kumita W., Henry R., Sakuma T., Ito R., Nozu R., Inoue T., Katano I., Sato K., Okahara N., Okahara J., Shimizu Y., Yamamoto M., Hanazawa K., Kawakami T., Kametani Y., Suzuki R., Takahashi T., Weinstein E.J., Yamamoto T., Sakakibara Y., Habu S., Hata J., Okano H., Sasaki E., 2016. Generation of a nonhuman primate model of severe combined immunodeficiency using highly efficient genome editing. Cell Stem Cell 19, 127-138.

Sato K.C., Tanji J., 1989. Digit-muscle responses evoked from multiple intracortical foci in monkey precentral motor cortex. J. Neurophysiol. 62, 959-970.

Solomon S.G., Rosa M.G., 2014. A simpler primate brain: the visual system of the marmoset monkey. Front Neural. Circuits 8, 96.

Soma S., Saiki A., Yoshida J., Ríos A., Kawabata M., Sakai Y., Isomura Y., 2017. Distinct laterality in forelimb-movement representations of rat primary and secondary motor cortical neurons with iIntratelencephalic and pyramidal tract projections. J. Neurosci. 37, 10904-10916.

Stüttgen M.C., Rüter J., Schwarz C., 2006. Two psychophysical channels of whisker deflection in rats align with two neuronal classes of primary afferents. J. Neurosci. 26, 7933-7941.

Stüttgen M.C., Schwarz C., 2008. Psychophysical and neurometric detection performance under stimulus uncertainty. Nat. Neurosci. 11, 1091-1099.

Thach W.T., 1968. Discharge of Purkinje and cerebellar nuclear neurons during rapidly alternating arm movements in the monkey. J. Neurophysiol. 31, 785-797.

Tachibana Y., Iwamuro H., Kita H., Takada M., Nambu A., 2011. Subthalamo-pallidal interactions underlying parkinsonian neuronal oscillations in the primate basal ganglia. Eur. J. Neurosci. 34, 1470-1484.

Takemoto A., Miwa M., Koba R., Yamaguchi C., Suzuki H., Nakamura K., 2015. Individual variability in visual discrimination and reversal learning performance in common marmosets. Neurosci. Res. 93, 136-43.

Takara S., Hatanaka N., Takada M., Nambu A., 2011. Differential activity patterns of putaminal neurons with inputs from the primary motor cortex and supplementary motor area in behaving monkeys. J. Neurophysiol. 106, 1203-1217.

Tanji J., Evarts E.V., 1976. Anticipatory activity of motor cortex neurons in relation to direction of an intended movement. J. Neurophysiol. 39, 1062-1068.

Tia B., Takemi M., Kosugi A., Castagnola E., Ansaldo A., Nakamura T., Ricci D., Ushiba J., Fadiga L., Iriki A., 2017. Cortical control of object-specific grasp relies on adjustments of both activity and effective connectivity: a common marmoset study. J. Physiol. Epub. ahead of print

Tokuno H., Tanaka I., 2011. Decision making and risk attitude of the common marmoset in a gambling task. Neurosci. Res. 71, 260-265.

Tokuno H., Watson C., Roberts A., Sasaki E., Okano H., 2015. Marmoset neuroscience. Neurosci. Res. 93, 1-2.

Tomioka I., Ishibashi H., Minakawa E.N., Motohashi H.H., Takayama O., Saito Y., Popiel H.A., Puentes S., Owari K., Nakatani T., Nogami N., Yamamoto K., Noguchi S., Yonekawa T., Tanaka Y., Fujita N., Suzuki H., Kikuchi H., Aizawa S., Nagano S., Yamada D., Nishino I., Ichinohe N., Wada K., Kohsaka S., Nagai Y., Seki K., 2017. Transgenic Monkey Model of the Polyglutamine Diseases Recapitulating Progressive Neurological Symptoms. eNeuro 4, 2.

Vitek J.L., Ashe J., DeLong M.R., Alexander G.E., 1994. Physiologic properties and somatotopic organization of the primate motor thalamus. J. Neurophysiol. 71, 1498-1513.

Vitek J.L., Bakay R.A., DeLong M.R., 1997. Microelectrode-guided pallidotomy for medically intractable Parkinson's disease. Advances in Neurology 74,183-198.

Wang X, Lu T, Snider RK, Liang L. 2005. Sustained firing in auditory cortex evoked by preferred stimuli. Nature 435, 341-346.

Welsh J.P., Lang E.J., Suglhara I., Llinás R., 1995. Dynamic organization of motor control within the olivocerebellar system. Nature 374, 453-457.

Yamada Y, Matsumoto Y, Okahara N, Mikoshiba K. 2016. Chronic multiscale imaging of neuronal activity in the awake common marmoset. Sci Rep. 6, 35722.

Yu H.H., Chaplin T.A., Egan G.W., Reser D.H., Worthy K.H., Rosa M.G., 2013 Visually evoked responses in extrastriate area MT after lesions of striate cortex in early life. J Neurosci. 33, 12479-12489.

7. Figure Legends

Figure 1. Marmoset head-fixation system.

A. A three-view drawing of a metal frame (a-c) and a marmoset chair (d-h). a, anterior-posterior stereotaxic bar; b, fixation block; c, metal frame; d, neck plate; e, waist plate; f, perch; g, waste tray; h, pillar. The neck plate can be tilted up to 30° to adjust positions of the marmoset's jaw and shoulders. **B**. Schematic diagram of a marmoset fixed to the head-fixation system. Units of numerical values in this figure are millimeter (mm).

Figure 2. Head-fixation tube, recording chamber, and mask for inhalational anesthesia.

A. A three-view drawing of the head-fixation tube. **B**. Two-view drawings of the recording chamber (left) and lid (right). **C**. Schematic diagram of the head-fixation tubes and recording chamber fixed to the marmoset's head. Units of numerical values in this figure are mm. **D.** A mask for inhalational anesthesia. **E.** A mouthpiece was inserted into the mouth through the mask and covered with a silicon rubber.

Figure 3. MRI scanning of the marmoset brain.

A. Stereotaxic MRI apparatus. a, supporting structure; b, stereotaxic MRI frame; c, fixation block; d, titanium rods; e, grid showing stereotaxic coordinates. **B**. An example of marmoset brain MRI (scanning from dorsal to ventral, sagittal plane 0.8 mm right from midline). Dorsal white dots represent a grid.

Figure 4. Neuronal recording and intracortical microstimulation (ICMS) mapping of the sensorimotor areas in the cerebral cortex.

A. Top view of the whole marmoset brain. The rectangle depicted on the right hemisphere shows the location of the mapping area in C. **B**. Single-unit firing in the primary motor cortex (MI). **C.** ICMS mapping of the right hemisphere (12 pulses, 200-μs duration, at 333 Hz). Each dot indicates a penetration site. Numerical values indicate the thresholds (in μA) to evoke movements by ICMS. Characters represent body parts with movements evoked by ICMS. Ak, ankle; Ch, chest; D, digit of forelimb; El, elbow; Ey, eyelid; hD, digit of hindlimb; hL, hindlimb; Hp, hip; Kn, knee; Sh, shoulder; UB, upper back; Wr, wrist; ×, no movements were evoked at less than 60 μA. The premotor cortex (PM), MI, and areas 3a and 3b could be identified based on their physiological features. The dotted lines indicate putative borders between these areas. **D**. A coronal section of the sensorimotor cortex of the marmoset. The cortex inside the inset rectangle was enlarged in E. D, dorsal; L, lateral. **E**. Enlarged view of the sensorimotor cortex. The border between the MI and area 3a defined electorophysiologically was indicated by a black arrow. The borders defined cytoarchitectonically were indicated by broken lines. **F**. The expressed GFP was clearly observed in the caudate nucleus. CC, corpus callosum; Cd, caudate nucleus; D, dorsal; M, medial.

Figure 5. Neuronal recordings in the deep brain structures.

The neuronal activities in the external (GPe) and internal (GPi) segments of the globus pallidus (**A**), thalamus (**B**), and deep cerebellar nucleus (CN; **C**).

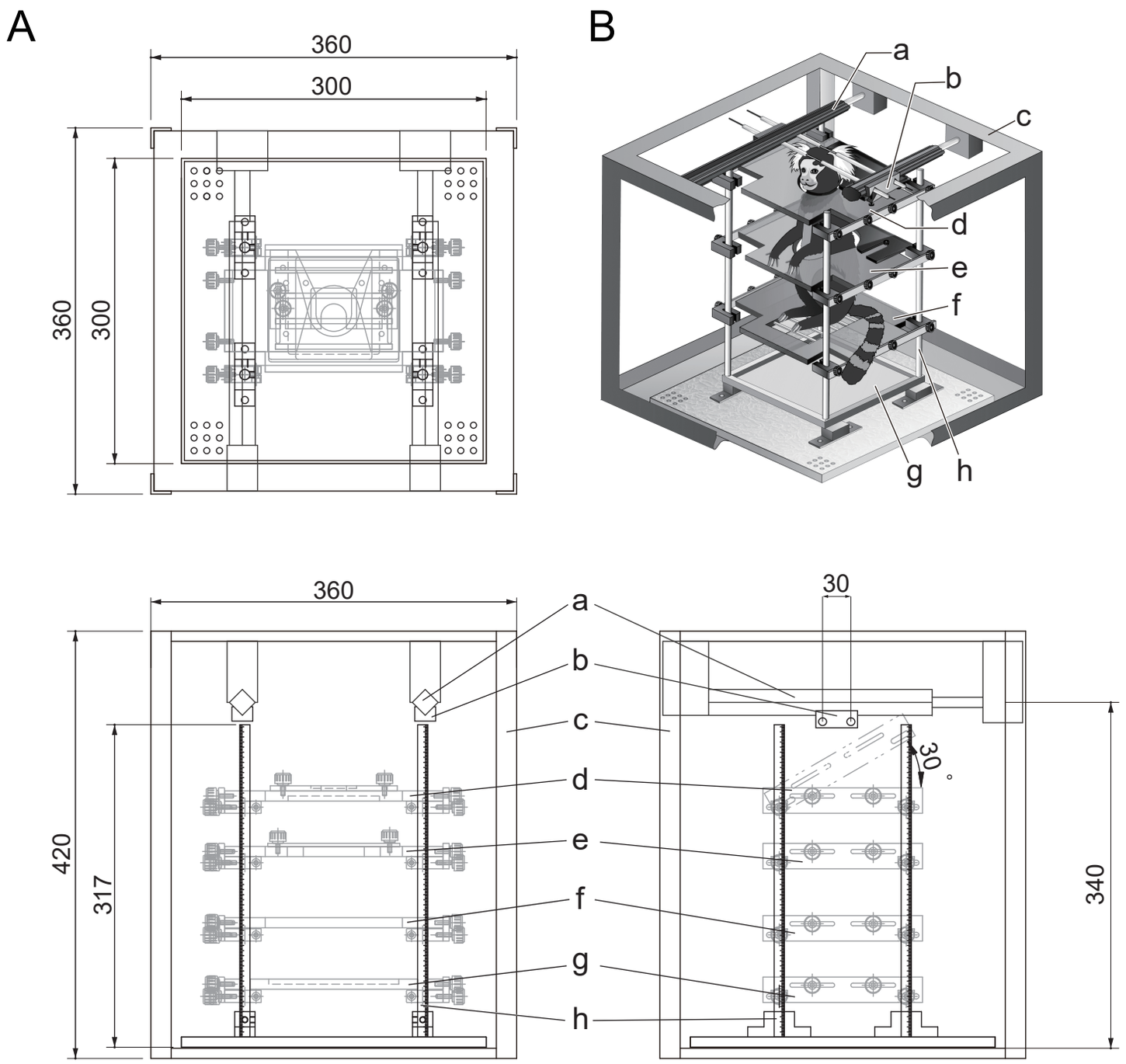

Figure 1.

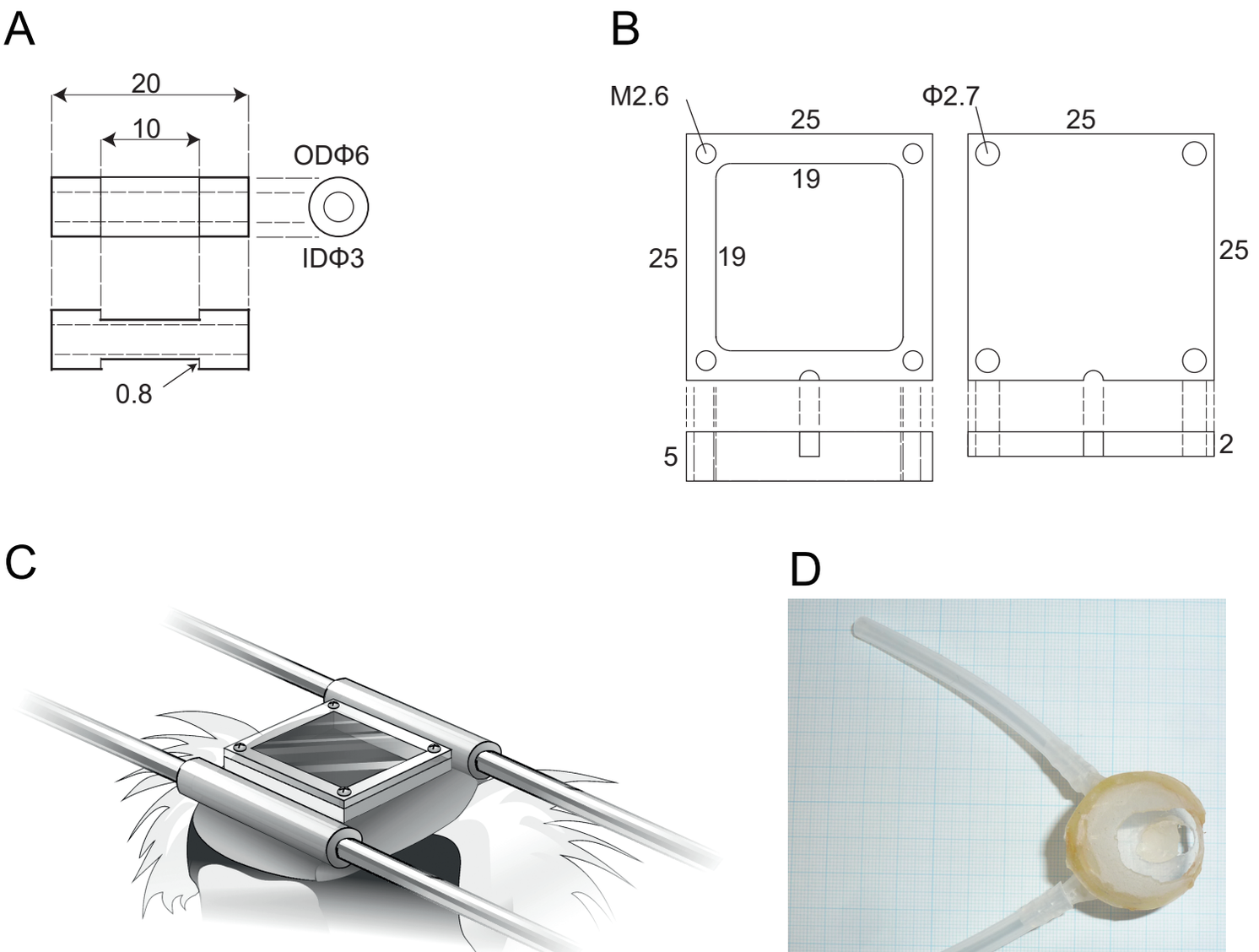

Figure 2.

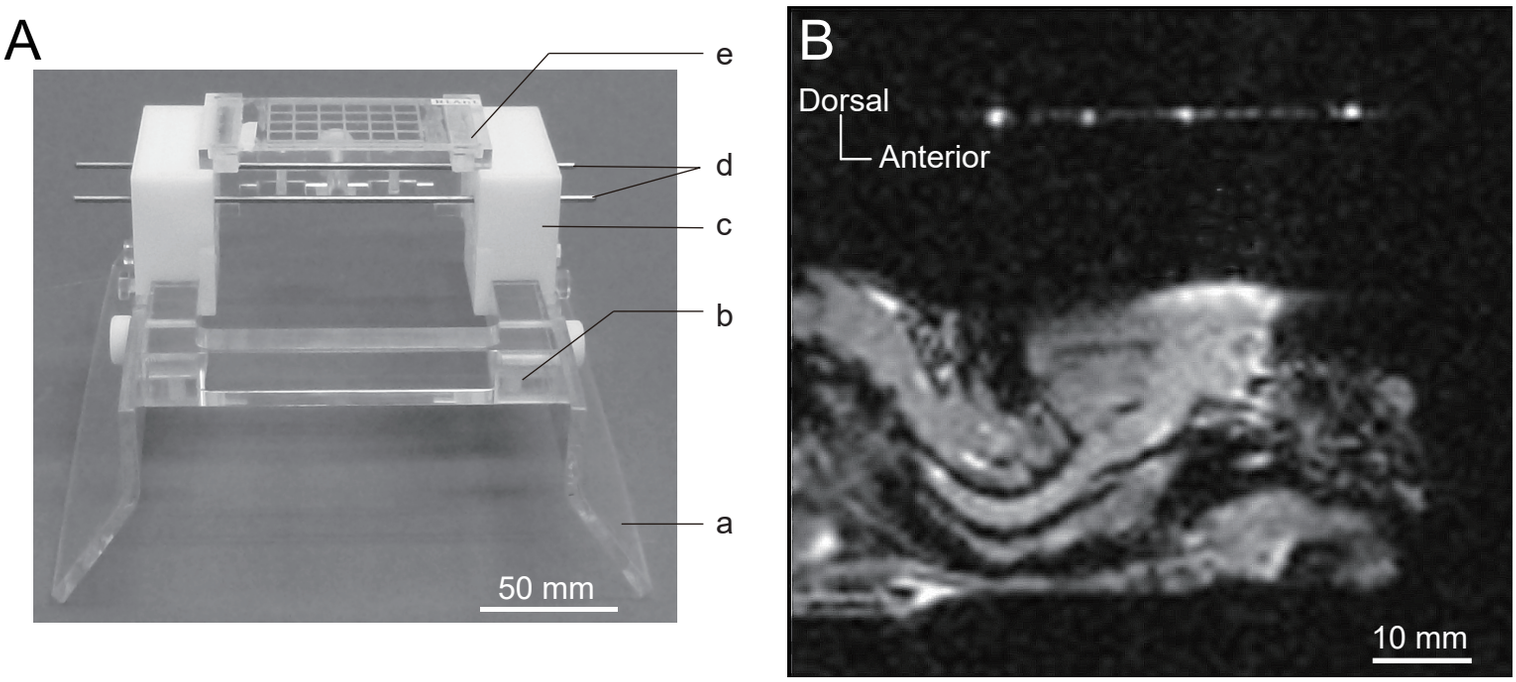

Figure 3.

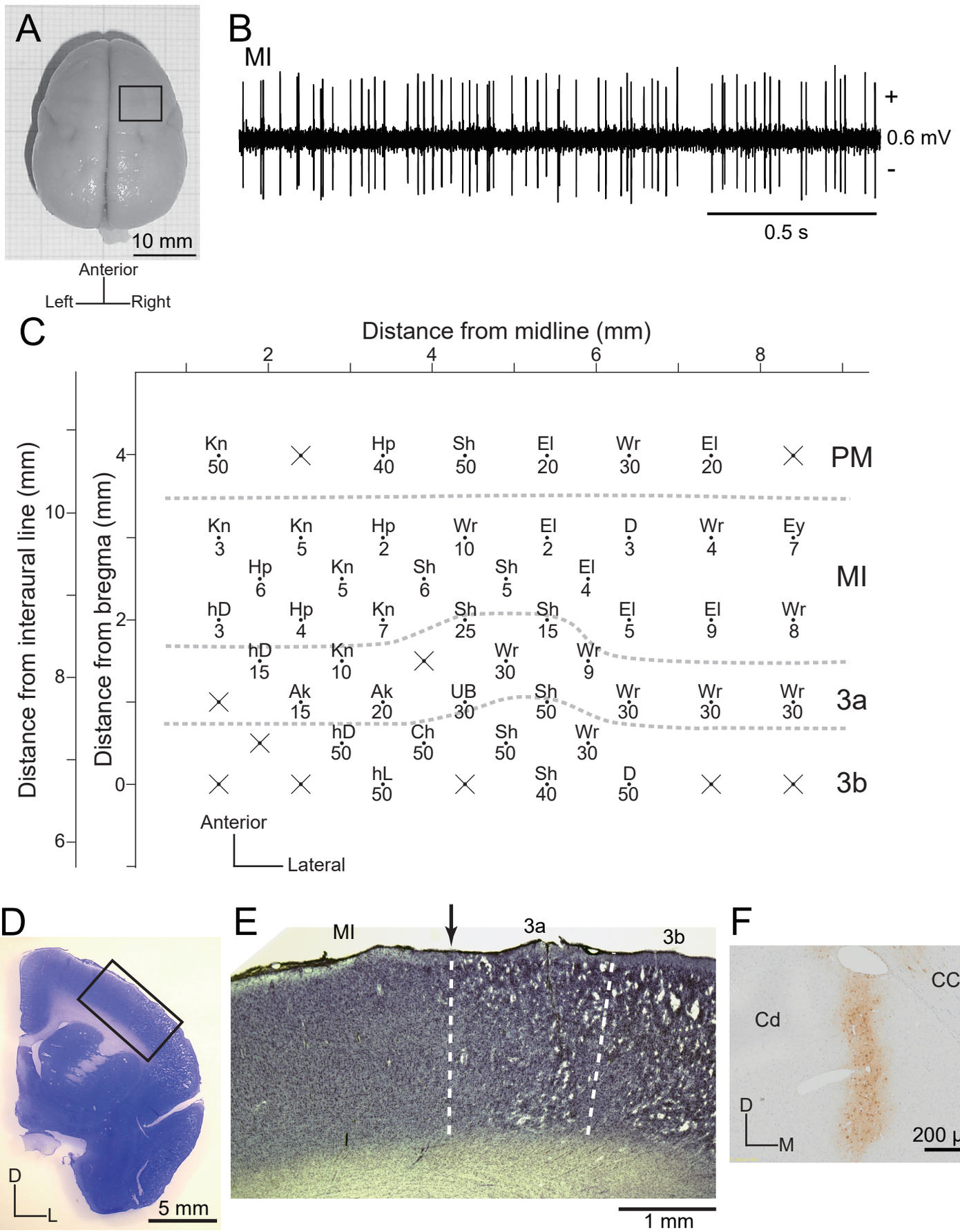
A
10 mm
Anterior
Left
Right
B
MI
+
0.6 mV
-
0.5 s
C
Distance from midline (mm)
2
4
6
8
Distance from interaural line (mm)
Distance from bregma (mm)
4
10
2
8
0
6
Kn 50
Hp 40
Sh 50
El 20
Wr 30
El 20
PM
Kn 3
Kn 5
Hp 2
Wr 10
El 2
D 3
Wr 4
Ey 7
Hp 6
Kn 5
Sh 6
Sh 5
El 4
MI
hD 3
Hp 4
Kn 7
Sh 25
Sh 15
El 5
El 9
Wr 8
hD 15
Kn 10
Wr 30
Wr 9
Ak 15
Ak 20
UB 30
Sh 50
Wr 30
Wr 30
Wr 30
3a
hD 50
Ch 50
Sh 50
Wr 30
hL 50
Sh 40
D 50
3b
Anterior
Lateral
D
D
L
5 mm
E
MI
3a
3b
I
1 mm
F
CC
Cd
D
M
200 µm

Figure 4.

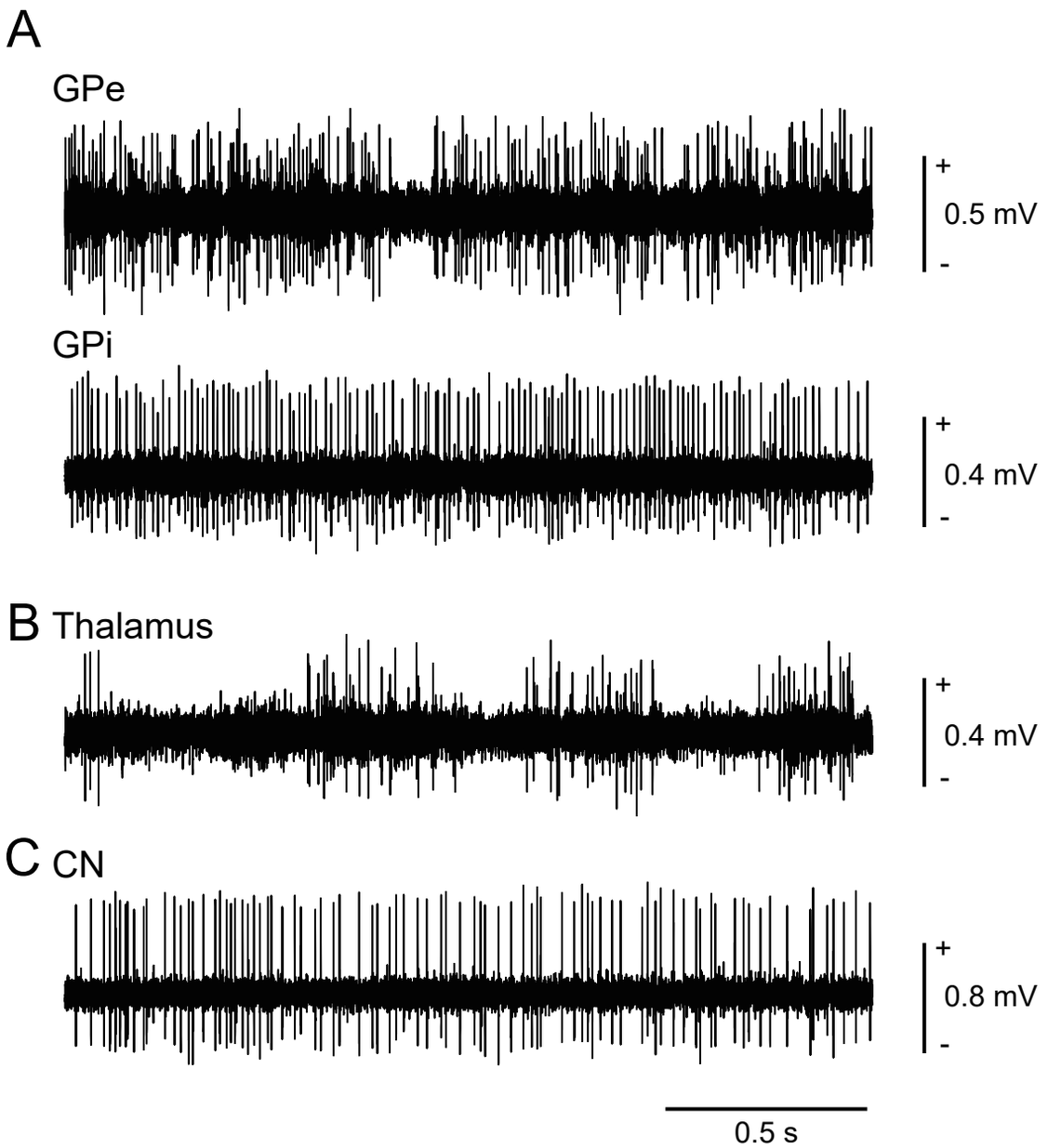

Figure 5.